Research Square

Preprints are preliminary reports that have not undergone peer review.
They should not be considered conclusive, used to inform clinical practice,
or referenced by the media as validated information.

Hierarchical polymer architectures governed by diffusion–reaction competition Decoupling morphology, packing and density in covalent systems

SATOSHI OKAMOTO

satoshi.okamoto.fv@riken.jp

RIKEN: Rikagaku Kenkyujo https://orcid.org/0009-0008-3901-6882

Justin Llandro

RIKEN: Rikagaku Kenkyujo https://orcid.org/0000-0002-1362-6083

Article

Keywords:

Posted Date: August 14th, 2026

DOI: https://doi.org/10.21203/rs.3.rs-10678262/v1

License: This work is licensed under a Creative Commons Attribution 4.0 International License.
Read Full License

Additional Declarations: Yes there is potential Competing Interest. S.O. is an inventor on a patent application related to the materials described in this work. All other authors declare no competing interests.

Hierarchical polymer architectures governed by diffusion–reaction competition

Decoupling morphology, packing and density in covalent systems

Satoshi Okamoto*[1,2,3] and Justin Llandro[2,3]

[1] *Materials and Structures Laboratory, Institute of Integrated Research, Institute of Science Tokyo, Yokohama, Kanagawa 226-8503, Japan*

[2] *RIKEN Baton Zone Program TRIP Headquarters, 2-1 Hirosawa, Wako 351-0198, Saitama, Japan*

[3] *Corporate Research Planning and Coordination Department, Sumitomo Chemical Co., Ltd., Japan, 2-7-1, Nihombashi, Chuo-ku, Tokyo, 103-6020, Japan*

*Correspondence:
Satoshi Okamoto (satoshi.okamoto.fv@riken.jp)

Abstract

Understanding how molecular systems encode higher-order structure remains a central challenge in chemistry. Here, we show that hierarchical architectures in covalent polymers are governed by the competition between reaction kinetics and mass transport, captured by an effective Damköhler number. Using phase-transition polymerization of C_3-symmetric monomers as a model system, we observe a continuous transition from lamellar flakes to solid spherical architectures with increasing reaction temperature.

Cross-sectional electron microscopy reveals that these apparently hollow-like particles are in fact fully solid, yet exhibit internal heterogeneity with a radially heterogeneous outer region and inner core. Despite pronounced morphological evolution, X-ray diffraction and density measurements show that molecular packing and bulk density remain essentially invariant, demonstrating a clear decoupling between morphology, packing and density.

Extending this analysis across chemically diverse monomer systems, we find that structural dimensionality can be consistently rationalized within an effective Damköhler-number framework rather than by chemical identity alone. These results establish a general diffusion–reaction framework for polymer assembly, in which chemical interactions are translated into structure through kinetic–transport competition. This work provides a conceptual basis for rationalizing and guiding the design of hierarchical polymer architectures by controlling the interplay between reaction and diffusion.

Introduction

Understanding how chemical systems generate higher-order structure from molecular components remains a central challenge in chemistry. While hierarchical architectures are ubiquitous across natural and synthetic materials, their formation is often interpreted as a direct consequence of chemical identity, intermolecular interactions or specific assembly pathways.[1,2] However, such descriptions rarely provide a general principle that predicts when and how structural dimensionality emerges. In many non-equilibrium systems, pattern formation is instead governed by the competition between reaction kinetics and mass transport, yet whether such kinetic–transport coupling can universally control structure formation in covalent polymer systems remains unclear. Establishing a framework that links molecular-level chemistry to emergent architecture through physically meaningful kinetic–transport descriptors is therefore a key unresolved problem.

Hierarchical and onion-like architectures are well established in inorganic systems, where diffusion-limited processes drive radial organization and curvature formation.[3-6] In contrast, the formation of comparable architectures in covalent polymer systems remains fundamentally unclear. Polymer materials differ fundamentally from inorganic systems in that molecular packing, chain growth, and structural organization are strongly influenced by reaction pathways and local mobility.[5] As a result, the relationship between reaction conditions and three-dimensional structure formation in polymers has yet to be established in a unified manner.

Aramid polymers, characterized by their rigid backbone and strong intermolecular hydrogen bonding, provide a particularly suitable platform for exploring such structure formation. Previous studies have demonstrated that phase-transition polymerization of aramid systems enables the formation of diverse morphologies, including lamellar and particulate structures, often with a high degree of molecular organization.[7-9] However, how these structures evolve into higher-dimensional architectures remains unresolved.

In many cases, spherical polymer particles exhibiting radial optical or electron contrast have been interpreted as hollow or core–shell structures based on indirect observations.[10-12] Furthermore, characterization of the internal structure of such polymer morphologies often relies on indirect observations, leaving open questions as to whether they adopt hollow or solid architectures. Another critical challenge is to identify a conceptual parameter that links reaction conditions to structural dimensionality and unifies diverse morphologies within a single kinetic–transport framework. In reaction–diffusion systems, the Damköhler number (Da), defined as the ratio between reaction kinetics and mass transport, provides a natural framework to describe pattern formation and structural evolution.[13] Although this concept has been successfully applied to

various physicochemical systems, its role in covalent polymer assembly has not been fully explored.

Here, we first investigate a single model system based on phase-transition polymerization of a C_3-symmetric aramid monomer (TTPA-IL), and demonstrate a temperature-driven structural evolution from lamellar flakes to spherical particles. Intermediate morphologies reveal aggregation and subsequent structural reorganization, indicating a continuous transition rather than discrete structure formation.

Cross-sectional FIB–SEM analysis confirms that these spherical particles are fully solid, excluding hollow structural models. Despite this, optical and electron microscopy reveal internal heterogeneity, suggesting non-uniform structural organization within the particles.

Importantly, true density measurements do not show significant changes despite morphological evolution, indicating that apparent morphology does not directly reflect internal packing or density.

These observations can be consistently interpreted within a Damköhler-number framework. Under low Da conditions, lamellar domains form and assemble through aggregation, whereas higher Da promotes reaction-driven inward growth and structural organization, leading to solid three-dimensional architectures.

Finally, we extend this analysis to multiple monomer systems with varying reactivity, demonstrating that diffusion–reaction competition provides a general framework for rationalizing dimensionality, morphology and packing density across the aramid and aromatic polyester systems investigated.

As illustrated in Figure 1, we hypothesize that increasing reaction temperature shifts the system from diffusion-dominated lamellar growth to reaction-driven inward growth, leading to solid spherical architectures.

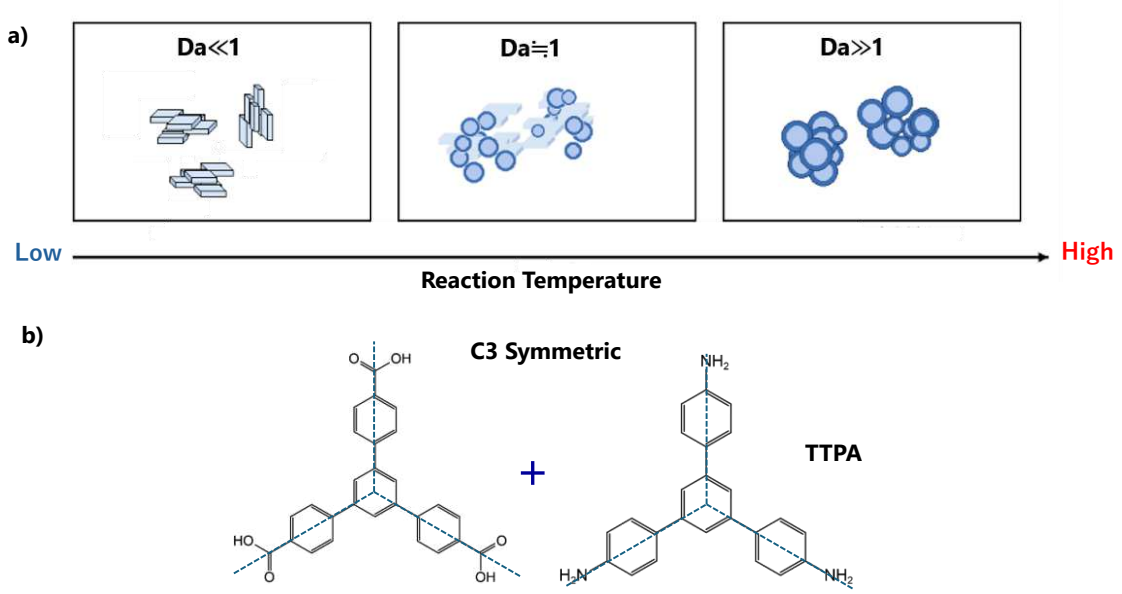


Figure 1 | Diffusion–reaction framework and molecular design.

(a) Conceptual illustration of structural evolution governed by the competition between reaction kinetics and mass transport, characterized by the Damköhler number (Da). Increasing temperature drives a transition from lamellar growth to inward growth, producing solid spherical architectures via intermediate aggregation and reorganization.

(b) Chemical structure of the C_3-symmetric aramid monomer (TTPA) employed in this study.

Here, we demonstrate that diffusion–reaction competition provides a unifying framework for three-dimensional structure formation in covalent aramid polymers. We first use a phase-transition polymerization of a C_3-symmetric aramid in an ionic liquid (TTPA–IL) as a model system and show that small changes in temperature induce a continuous evolution from lamellar flakes to spherical particles via intermediate aggregation and deformation. Cross-sectional electron microscopy reveals that these apparently hollow-like spheres are in fact fully solid yet internally heterogeneous, with radially organized outer regions and disordered cores. X-ray diffraction and true density measurements further demonstrate that local packing distance and bulk density remain nearly invariant during this transition, establishing a clear decoupling between external morphology, molecular packing, and internal organization. We then extend this analysis to chemically diverse monomer chemistries with different effective reactivities and construct an effective Damköhler-number map that consistently links reaction conditions to structural dimensionality. Together, these results establish a general diffusion–reaction framework for hierarchical architecture formation in covalent polymers.

Results

Temperature-driven morphological evolution in a model aramid system

We first establish a temperature-driven morphological transition in a model aramid system, in which lamellar flakes continuously evolve into spherical particles via intermediate aggregation and deformation. As a representative platform, we focus on phase-transition polymerization of a C_3-symmetric aramid monomer in an ionic liquid (TTPA–IL), where the growing polymer undergoes a solvent-induced phase separation that couples chain growth to mesoscale structure formation. In this system, temperature serves as an experimental knob that simultaneously affects reaction kinetics and mass transport, effectively tuning the balance between diffusion and reaction and thus the effective Damköhler number.

Figure 2 summarizes the morphology of the polymerization products obtained at 150, 180, and 200 °C. At 150 °C, polarized optical microscopy (POM) reveals extended birefringent domains, which are resolved by scanning electron microscopy (SEM) into flake-like lamellar structures with pronounced lateral growth. These lamellae form large, interconnected domains that reflect diffusion-dominated growth under relatively mild reaction conditions.

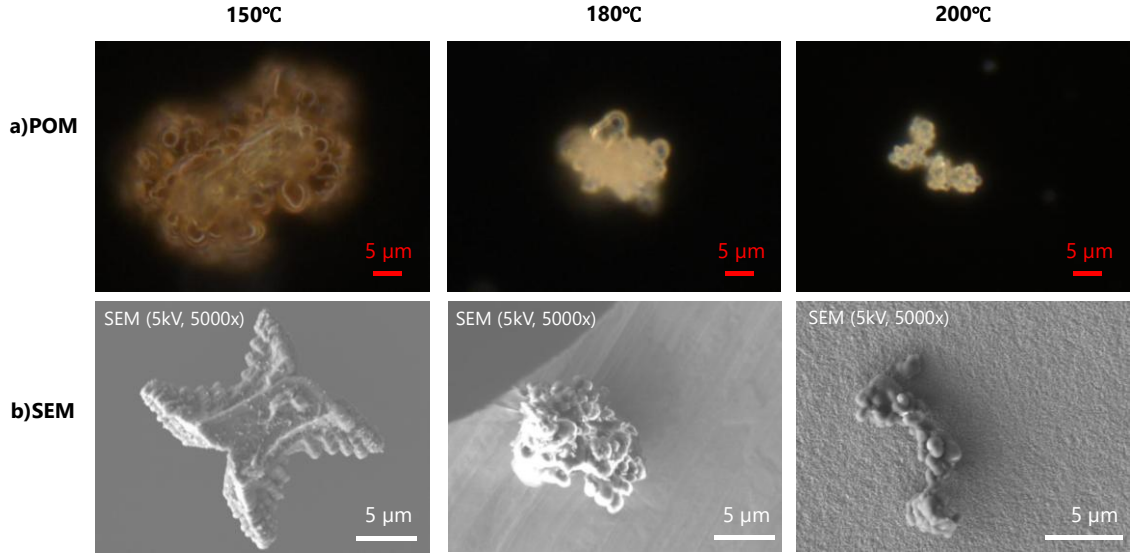


Figure 2 | Temperature-dependent structural evolution in TTPA-IL.

(a) Polarized optical microscopy (POM) and (b) scanning electron microscopy (SEM) images of polymerization products obtained at 150, 180, and 200 °C. A continuous transition from lamellar flakes to spherical particles is observed with increasing temperature.

Upon increasing the temperature to 180 °C, intermediate morphologies emerge that bridge the lamellar and particulate states. POM images show fragmented domains, while

SEM reveals partially aggregated, deformed lamellae in which sharp edges coexist with curved segments. Some objects retain plate-like features indicative of aggregated flakes, whereas others exhibit partially fused, bent, or rolled morphologies, suggesting that lamellae undergo progressive aggregation followed by structural reorganization. The coexistence of these features demonstrates that the transition proceeds through a continuum of intermediate states rather than discrete, well-separated morphologies.

At 200 °C, the morphology is dominated by well-defined spherical particles with smooth outer surfaces. The lamellar textures observed at lower temperatures are no longer apparent, and the particles appear as isolated or loosely aggregated spheres in both POM and SEM images.

This temperature-dependent series thus reveals a continuous evolution from two-dimensional lamellar flakes to three-dimensional spherical architectures, showing that small changes in temperature – and therefore in the balance between diffusion and reaction – are sufficient to switch the dominant growth mode from lateral lamellar extension to three-dimensional particle formation.

Solid yet heterogeneous internal architecture

The temperature-driven transition from lamellar flakes to spherical particles raises a central question about the internal architecture of the resulting three-dimensional structures. Spherical polymer particles with radial contrast are often interpreted as hollow or core–shell structures based solely on optical or electron microscopy images, yet direct evidence for their internal organization is scarce. To clarify whether the particles are hollow, porous, or fully solid, and how their internal structure evolves with temperature, we examined their interiors by a combination of scanning transmission electron microscopy in SEM mode (STEM–SEM) and focused ion beam–scanning electron microscopy (FIB–SEM).

STEM–SEM images (Figure 3) of particles obtained at different temperatures reveal pronounced contrast variations within individual objects, indicative of non-uniform internal organization. At intermediate temperatures, particles that retain partially lamellar outlines exhibit bright and dark regions consistent with domains of distinct internal organization, whereas fully spherical particles display a radial contrast gradient between the outer shell and the interior. Such patterns cannot be explained by a homogeneous density distribution and instead suggest the presence of heterogeneous structural domains within a continuous solid matrix. These observations are consistent with a growth mechanism in which lamellae first aggregate and then progressively reorganize under non-equilibrium conditions, giving rise to spatially heterogeneous internal

organization.[11,12]

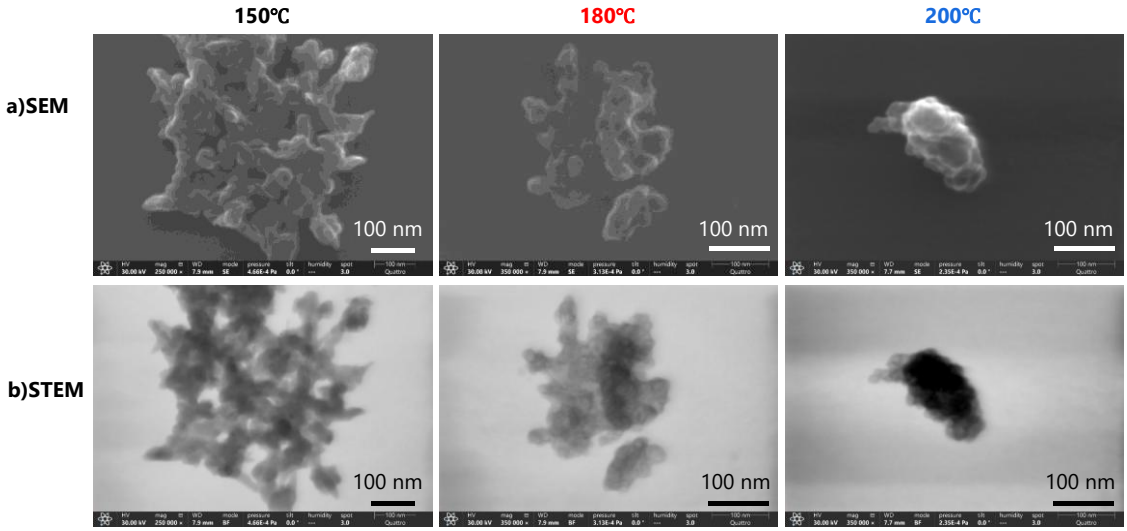


Figure 3 | Internal structural heterogeneity of TTPA-IL

STEM--SEM images of particles obtained at different temperatures, showing internal contrast consistent with spatially heterogeneous internal organization. The contrast may reflect variations in molecular orientation, mesoscale order and/or local composition; its precise origin remains unresolved.

To directly determine whether these particles are hollow or solid, we performed cross-sectional analysis using FIB–SEM (Figure 4). Individual particles were sectioned along their diameter and imaged at low acceleration voltage to minimize beam damage and enhance internal contrast. The cross-sections reveal that the particles are fully solid across their entire volume, with no detectable voids or central cavities. Instead, the interior appears densely filled, while subtle contrast differences persist between the outer regions and the core, reflecting the internal heterogeneity inferred from STEM–SEM. These cross-sections exclude a hollow interior and instead reveal a continuous solid particle with heterogeneous internal contrast.

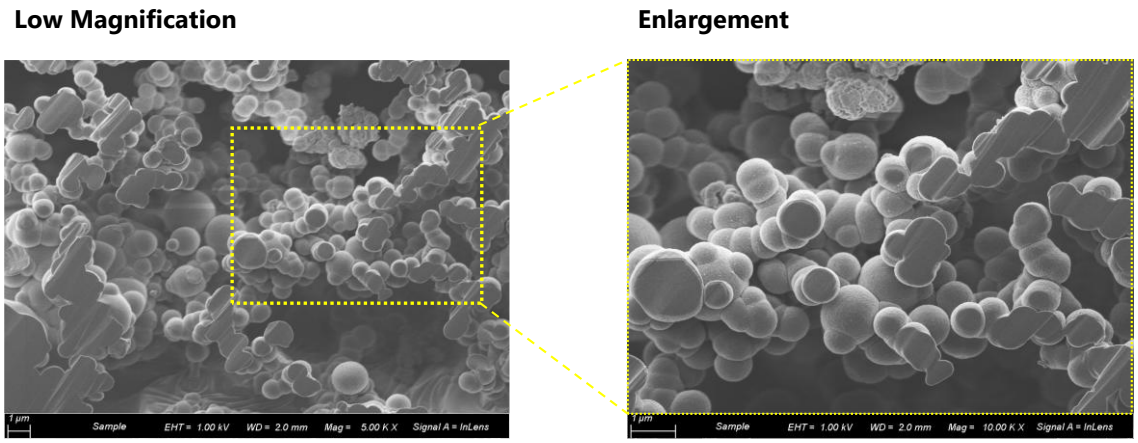


Figure 4 | Solid internal structure revealed by cross-sectional analysis of TTPA-IL

FIB–SEM cross-sectional images of polymer particles. The left panel shows a low-magnification overview of the entire particle, while the right panel displays a magnified view of a selected region. This analysis confirms that the particles are fully solid without internal voids, while revealing internal structural heterogeneity.

Together, the STEM–SEM and FIB–SEM analyses demonstrate that the apparently hollow-like onion architectures in this aramid system are, in fact, solid particles with heterogeneous internal organization.[10] The outer regions are structurally distinct from the interior, yet the material is continuous throughout the particle. This establishes a solid but internally heterogeneous architecture as the basis for the subsequent analysis of molecular packing, density, and mesoscale internal organization, and motivates the need to decouple morphology from intrinsic packing properties in the following sections.

Mesoscale structural organization revealed by SAXS

To probe structural organization beyond the molecular packing scale, small-angle X-ray scattering (SAXS) measurements were performed on TTPA–IL.

The SAXS profile exhibits distinct scattering maxima at q = 0.0516, 0.101, and 0.208 $Å^{-1}$, corresponding to characteristic spacings of ($d = 2\pi/q$) of approximately 12.2, 6.2, and 3.0 nm, respectively (Figure 5).

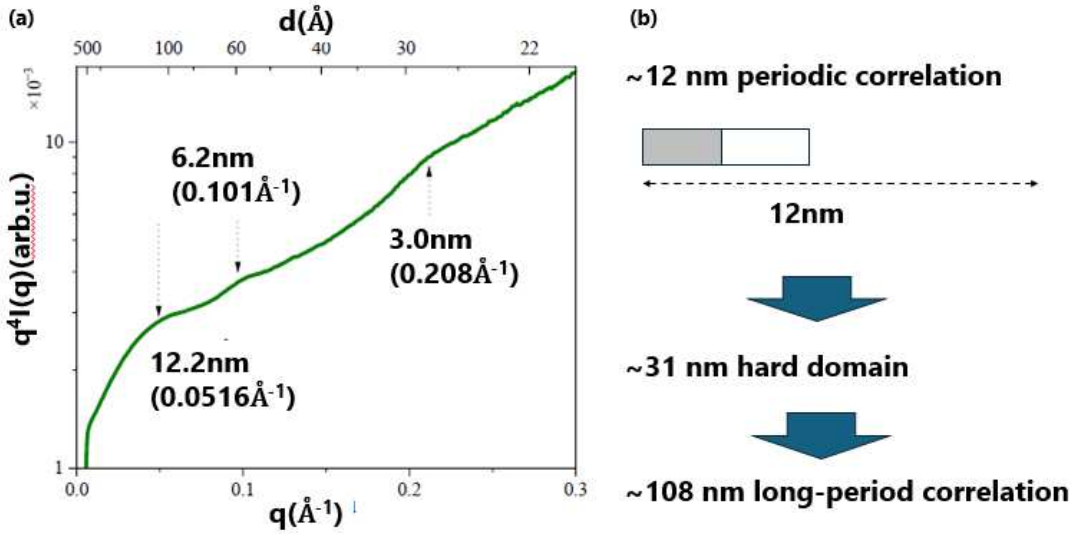


Figure 5 | Hierarchical mesoscale structural correlations revealed by SAXS.

(a) SAXS profile of TTPA–IL showing characteristic spacings of approximately 12.2, 6.2 and 3.0 nm, corresponding to scattering maxima at q = 0.0516, 0.101 and 0.208 $Å^{-1}$, respectively. The near 1:2:4 relationship suggests periodic structural correlations at nanometer length scales.

(b) Schematic representation of possible hierarchical correlations suggested by SAXS. A characteristic periodic correlation of approximately 12 nm is incorporated into larger hard domains (~31 nm), while correlation-function analysis further indicates a long-period correlation of approximately 108 nm across multiple mesoscale length scales.

These reflections occur at nearly 1:2:4 ratios in reciprocal space, suggesting characteristic structural correlations on the ~10 nm length scale, although the precise structural origin of these reflections remains unresolved.

The observed periodicities are substantially larger than the expected intermolecular packing distance of aromatic polyamides (~4.3 Å), indicating that the SAXS reflections originate from mesoscale organization rather than local molecular packing.

Correlation-function analysis further yielded a weak periodic structure with a characteristic hard-domain size of approximately 31 nm and a long-period spacing of approximately 108 nm (Supplementary Figure S1), indicating that the ~12 nm periodic correlations are incorporated into larger hierarchical structural domains, consistent with approaches commonly used in small-angle scattering analyses of hierarchical materials. [14] The surface of the periodic domains (at the mesoscale) appears to be relatively rough, as indicated by the power-law dependence observed in the q-range of 0.0073–0.187 $Å^{-1}$ as shown in Figure 6. [14-16].

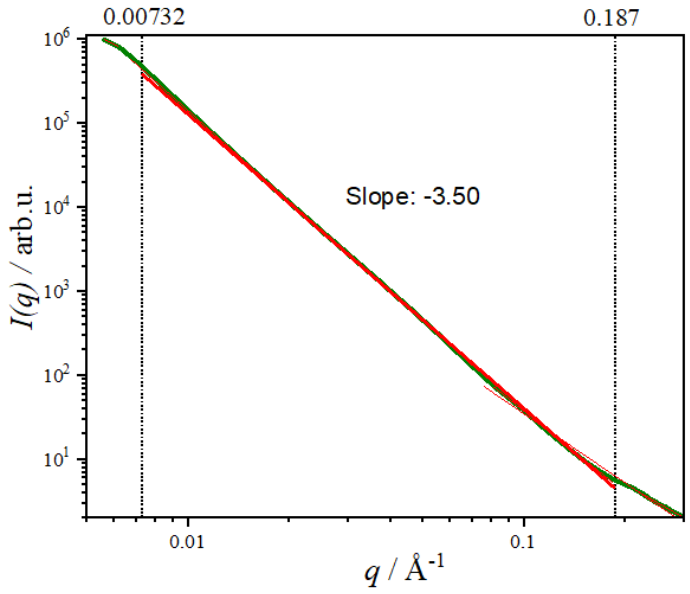


Figure 6 Log-log plot of SAXS data. Slope value represents the rough surface as I(q) α q^{-m}, with *m* = 3.50.

Together with the STEM–SEM and FIB–SEM observations, these results demonstrate that the apparently solid TTPA–IL particles possess hierarchical internal organization spanning multiple length scales, from molecular packing (~0.4 nm) to mesoscale periodic correlations (~12 nm) and larger structural domains (>30 nm).

The characteristic domain size estimated from SAXS (~31 nm) is comparable to the spatial scale of the contrast heterogeneities observed in STEM–SEM images. Although a direct one-to-one correspondence cannot be established at present, this agreement suggests that the SAXS-derived domains may reflect the heterogeneous internal organization visualized by electron microscopy.

Decoupling morphology, mesoscale organization and molecular packing

Although SAXS reveals structural correlations extending from several nanometers to over one hundred nanometers, PXRD measurements show that the local intermolecular packing distance remains essentially unchanged throughout the structural evolution.

The solid yet heterogeneous architecture of the spherical particles suggests that external morphology may be decoupled from local molecular packing and overall density. To test this hypothesis, we combined powder X-ray diffraction (PXRD) and true density measurements for samples prepared at different reaction temperatures. These measurements probe, respectively, the local packing motif of the polymer chains and the average density of the bulk material, allowing us to assess whether the transition from

lamellar flakes to spherical particles involves significant changes in intrinsic packing. PXRD patterns of the TTPA–IL system exhibit broad reflections corresponding to an interlayer spacing of approximately 4.3 Å over the entire temperature range investigated (Figure 6).

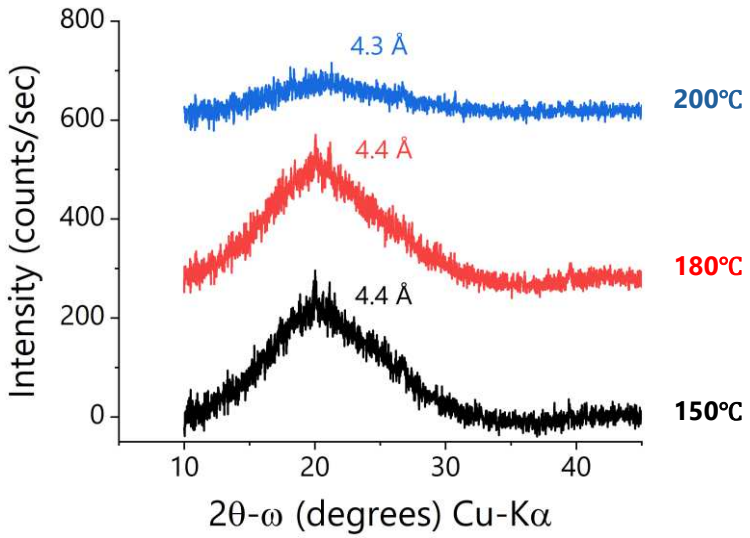


Figure 6 | Molecular packing revealed by X-ray diffraction.
PXRD patterns showing interlayer spacings of ~4.3 Å, indicating that local molecular packing is largely preserved during the structural transition.

The peak positions remain essentially unchanged as the morphology evolves from extended lamellae at 150 °C to spherical particles at 200 °C, indicating that the local packing motif of the aromatic polyamide backbone is largely preserved during structural evolution. Although peak intensities and widths show minor variations that may reflect subtle differences in coherence length or defect density, the characteristic interlayer spacing does not display any systematic dependence on temperature. This invariance implies that the polymer chains maintain a similar packing distance regardless of whether the material adopts a lamellar or particulate morphology.

True density measurements obtained by helium pycnometry reveal a similarly weak dependence on reaction temperature (Figure 7).

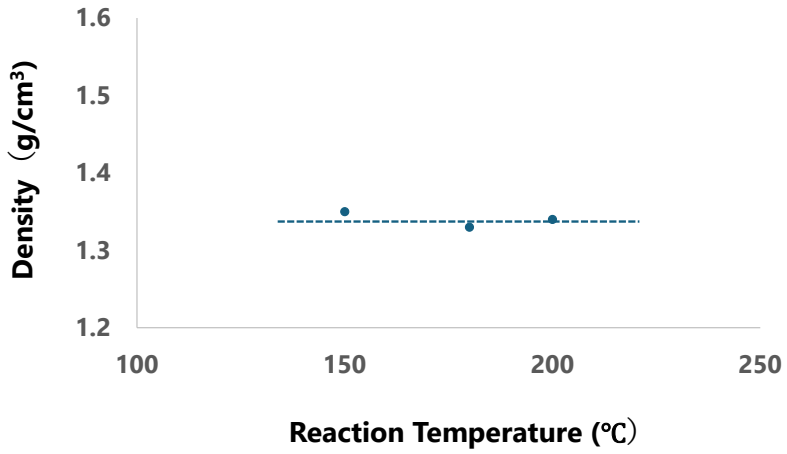


Figure 7 | Temperature-dependent density evolution of TTPA-IL.

True density measured by helium pycnometry as a function of reaction temperature, showing that density remains nearly constant during the transition.

This behavior stands in stark contrast to the strong contrast variations observed in electron microscopy, which commonly suggest hollow or porous architectures. The combination of constant interlayer spacing, nearly invariant density, and solid interiors therefore reveals a clear decoupling between external morphology and intrinsic packing properties. The observed contrast is unlikely to arise solely from macroscopic void formation or bulk-density differences. Instead, it is consistent with spatially heterogeneous internal organization, potentially involving differences in molecular orientation, mesoscale ordering and/or local composition. This motivates a proposed structural picture in which non-equilibrium growth may generate a radial gradient in internal organization within a mechanically continuous solid, as schematically illustrated in Figure 8.

Interestingly, the additional level of structural organization revealed by SAXS is not captured by either PXRD or density measurements. Together, PXRD and SAXS indicate hierarchical organization extending across multiple length scales, from invariant molecular packing to well-defined mesoscale correlations. This observation reinforces the decoupling between morphology, packing, density, and mesoscale organization.

Although the precise structural origin remains unresolved, the coexistence of invariant molecular packing, nearly constant bulk density, and well-defined SAXS correlations suggests that mesoscale organization can evolve independently of both local packing and overall density.

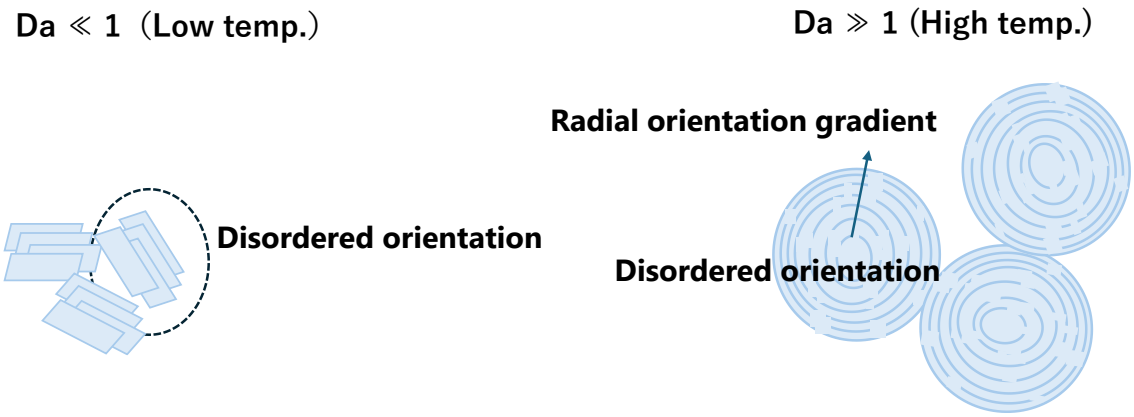


Figure 8 | Proposed diffusion–reaction mechanism and evolution of internal organization. Low effective-Da conditions are proposed to favour laterally extended lamellar growth with comparatively uniform internal organization. At higher effective Da, rapid reaction relative to transport is proposed to promote inward growth and spatially heterogeneous internal organization. The radial organization shown is a mechanistic model consistent with the observed morphology and contrast, rather than a direct measurement of molecular orientation.

Generality across monomer chemistries

The results above establish a decoupling of morphology, mesoscale organization, molecular packing, and density in a single model aramid system. To test whether this behavior reflects a more general principle, we next examined a series of monomer chemistries with systematically varied reactivity and interaction strengths. The systems include amide-based monomers (TPA, TPMA) and ester-based monomers (TPE, TTPE), covering a wide range from highly reactive combinations to lower-reactivity controls (Figure 9).

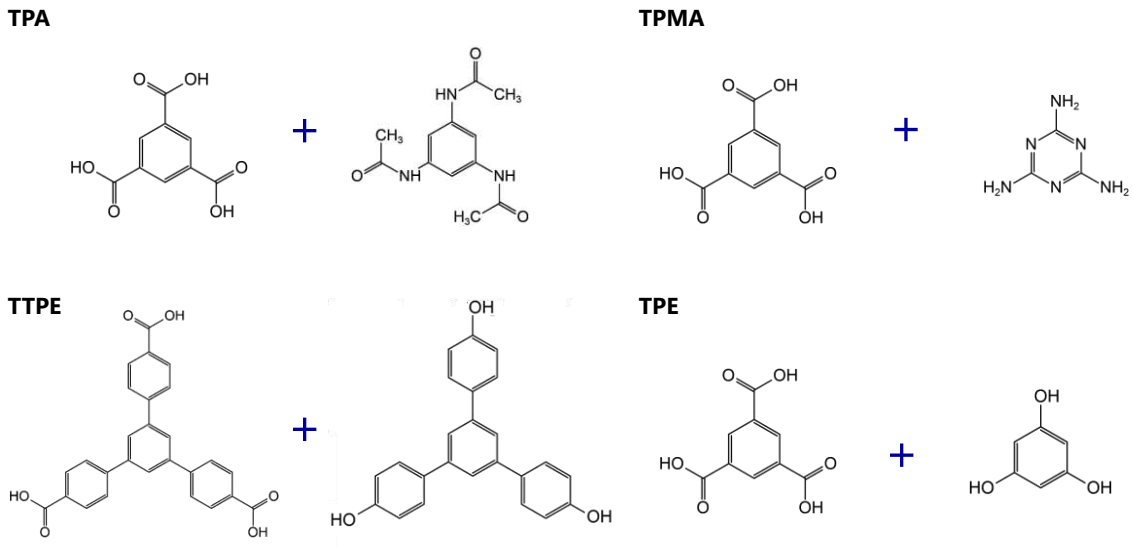


Figure 9 | Chemical diversity of monomer systems used in this study.

Chemical structures of representative monomer systems investigated, including amide-based (TPA, TPMA) and ester-based (TPE, TTPE) chemistries.

All systems were subjected to analogous phase-transition polymerization conditions in ionic liquid or high-boiling solvent, enabling a comparative assessment of structural dimensionality under diffusion–reaction-controlled growth.

The chemical structures of the representative monomers are summarized in Figure 9, while the corresponding morphological and structural data are provided in the Supplementary Information (Figures S2–S6). Highly reactive systems such as TPA and TTPE reproducibly form three-dimensional architectures, including spherical or aggregated particulate structures, analogous to the TTPA–IL case. In contrast, less reactive systems such as TPE (phloroglucinol-based ester) and TPMA (melamine-based amide) yield predominantly planar lamellar flakes with limited tendency toward three-dimensional growth. This systematic trend indicates that structural dimensionality correlates strongly with effective reactivity and growth kinetics, rather than with specific chemical identity.

Further analysis of interlayer spacing and density across these systems reveals additional insight into the underlying packing principles. As summarized in Figure S6, density exhibits an approximately inverse correlation with interlayer distance, which appears nearly linear over the observed range as a first-order approximation. Separating ester and amide systems reveals a small systematic offset between the two classes, suggesting that differences in packing efficiency and intermolecular interactions contribute to modest variations in density at a given spacing. Nevertheless, the overall trend indicates that

packing density is primarily governed by local interchain interactions, while structural dimensionality is controlled by kinetic–transport competition.

These observations show that chemically diverse monomers conform to the same qualitative framework: highly reactive systems, which favor rapid bond formation relative to diffusion, are more likely to develop three-dimensional architectures, whereas less reactive systems remain confined to two-dimensional lamellar growth. The fact that this behavior spans both amide and ester chemistries underscores that the governing factor is not the specific functional group, but rather the balance between reaction kinetics and mass transport. This generality supports the view that diffusion–reaction competition provides a unifying mechanism linking structural dimensionality to formation conditions in covalent polymer systems.

Diffusion–reaction framework and unified Da map

The temperature-dependent morphological evolution in TTPA–IL and the systematic behavior across multiple monomer chemistries suggest that an effective kinetic–transport descriptor can organize the principal trends in structure formation in these systems. In classical reaction–diffusion theory, the Damköhler number (Da), defined as the ratio of the characteristic reaction rate to the characteristic diffusion rate, provides a natural measure of the competition between kinetics and mass transport. Here, we adopt Da as an effective parameter that encapsulates the balance between bond formation and species mobility during phase-transition polymerization, and use it as a conceptual axis to organize the experimental results.

Figure 10 presents a unified map that links structural dimensionality to the effective Damköhler number in polymer systems.

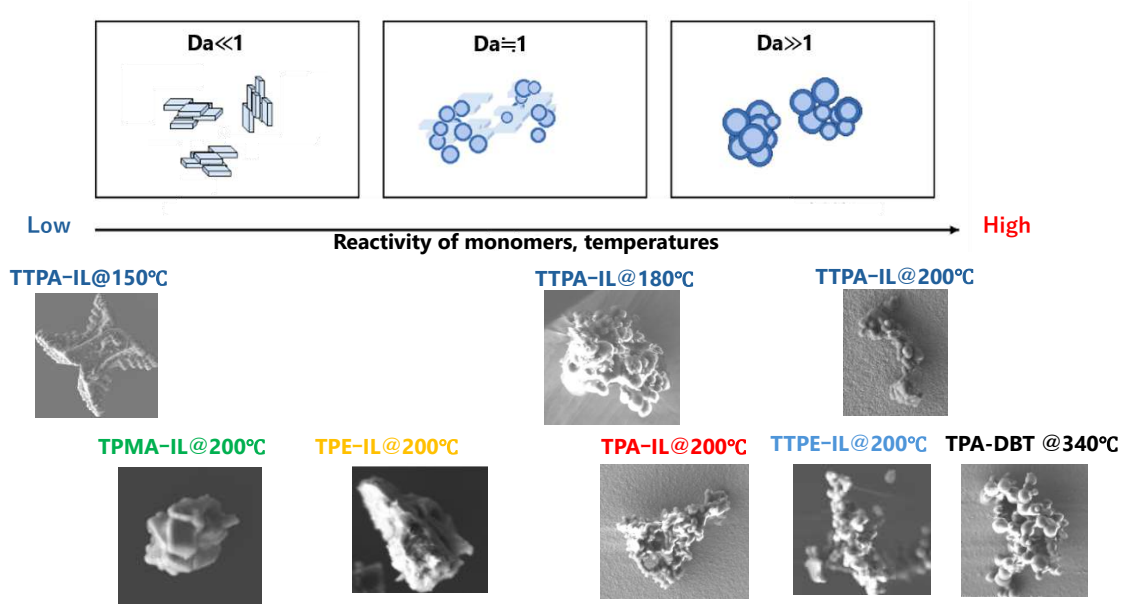


Figure 10 | Unified map of diffusion–reaction-controlled structure formation.
Schematic diagram illustrating the relationship between the Damköhler number (Da) and structural dimensionality in polymer systems. A continuous transition from two-dimensional lamellar structures to solid three-dimensional architectures is observed with increasing Da, corresponding to a shift from diffusion-dominated to reaction-dominated regimes. This framework unifies results obtained from temperature variation and different monomer systems, demonstrating that structural evolution can be consistently interpreted within a diffusion–reaction framework across chemically diverse systems.

Importantly, this map unifies results obtained from both temperature variation in the TTPA–IL system and from chemically diverse monomer chemistries. Temperature changes in a single system are expected to alter the effective kinetic--transport balance by modifying both reaction kinetics and mass transport, while monomer reactivity and interaction strength are expected to shift the effective kinetic–transport balance by altering intrinsic kinetics and phase-separation behaviour. In both cases, the observed structural dimensionalities can be qualitatively organized along the same effective-Da axis, suggesting that diffusion--reaction competition is a dominant descriptor of the transition alongside chemical interactions.

We emphasize that the Da values in this study are treated as effective parameters, and Figure 10 should be viewed as a conceptual representation rather than a strictly quantitative phase diagram. Although treated as an effective parameter, the Damköhler number provides a conceptual organizing axis that relates reaction conditions to the observed structural dimensionality. This effective Da map provides a design-oriented framework for rationalizing hierarchical polymer architectures through the balance

between reaction and mass transport.

Discussion

The present results establish a unified framework for structural dimensionality in covalent polymer systems governed by the competition between reaction kinetics and mass transport.[13] By systematically varying temperature and monomer chemistry, we show that structural dimensionality, from two-dimensional lamellae to three-dimensional solid architectures, can be rationalized in terms of an effective Damköhler number that captures the balance between bond formation and species mobility.[13] This diffusion–reaction framework extends concepts traditionally applied to inorganic onion-like materials and classical reaction–diffusion systems to covalently bonded polymers, revealing how non-equilibrium processes can be harnessed to control both morphology and internal organization.[1–6,13]

SAXS further revealed structural correlations at intermediate length scales that bridge molecular packing and particle morphology. Characteristic periodic correlations at approximately 12 nm, together with larger hard domains (~31 nm) and long-period correlations (~108 nm), demonstrate that internal organization extends across multiple hierarchical length scales. The coexistence of invariant PXRD spacing, nearly constant density, and well-defined SAXS correlations further supports the decoupling of local packing from mesoscale structural organization. The origin of the ~12 nm periodic correlation remains unclear. One plausible interpretation is that the polymer–ionic liquid composite develops nanoscale compositional heterogeneity during phase-transition polymerization, giving rise to periodic electron-density contrasts detected by SAXS. Under this scenario, the ~31 nm hard domains and ~108 nm long-period correlations may represent higher-order structural organization built upon the fundamental ~12 nm periodicity.

At present, the available SAXS data do not permit an unambiguous structural assignment of these correlations. Nevertheless, the observed features consistently indicate the presence of hierarchical organization extending over multiple mesoscopic length scales.

A key insight of this study is the clear decoupling between external morphology, mesoscale organization, molecular packing, and bulk density. Despite the pronounced transition from lamellar flakes to spherical particles, both the interlayer spacing and the true density remain nearly invariant, indicating that the intrinsic packing motif of the aromatic polyamide network is preserved across these architectures. At the same time, electron microscopy reveals strong radial contrast and internal heterogeneity within fully solid particles, demonstrating that apparent hollow-like morphologies do not necessarily

imply a hollow interior or an appreciable change in bulk density. The nearly invariant PXRD spacing further indicates that this morphological transition occurs without an appreciable change in the average local packing distance. The observations are consistent with non-equilibrium growth under high effective-Da conditions generating radially heterogeneous internal organization and onion-like contrast within a continuous solid.[13]

This decoupled view contrasts with conventional interpretations in polymer and colloid science, where spherical objects with radial contrast are often modeled as hollow capsules or classical core–shell particles.[6,10-12] The combined STEM–SEM and FIB–SEM analysis presented here shows that such interpretations can be misleading when based solely on indirect imaging, and that spatially heterogeneous internal organization can play an important role in determining contrast and apparent architecture. The present results therefore highlight the importance of direct cross-sectional imaging for correctly identifying internal structure, and they suggest that solid, internally heterogeneous architectures may be more prevalent in polymer systems than previously recognized despite the widespread use of hollow and core–shell structural models in polymer particle research.[10-12].

The generality of the diffusion–reaction framework across chemically diverse monomer systems further underscores that structural dimensionality is primarily dictated by kinetic–transport competition rather than chemical identity.[13] Highly reactive systems, which favor rapid bond formation and early phase separation, access high effective Da regimes that promote inward growth and three-dimensional structure formation. Less reactive combinations, in contrast, remain in diffusion-dominated regimes where growth proceeds laterally, yielding stable lamellar flakes even under extended reaction conditions. This behavior is observed for both amide and ester chemistries, with packing density largely set by local interchain interactions, as reflected in the correlation between interlayer spacing and density. These findings suggest a design strategy in which monomer reactivity and interaction strength are tuned to control Da and, consequently, structural dimensionality, while local packing is adjusted independently through molecular design.[13]

The diffusion–reaction map developed here provides a conceptual link between covalent polymer systems and a broader class of reaction–diffusion-driven structures, including inorganic onion-like materials and hierarchical assemblies in soft matter.[1–6] In inorganic systems, curvature and multilayer formation are often attributed to diffusion-limited growth and anisotropic surface energies,[1–6] whereas in the present polymer systems, analogous behavior emerges from the coupling of chain growth, phase

separation, and constrained mobility under high Da conditions.[13] This parallel suggests that similar kinetic–transport principles may underlie hierarchical structure formation across disparate material classes, from atomic-scale graphitic onions to macromolecular networks, and that effective parameters such as Da can serve as unifying descriptors for these phenomena. [1–6,13]

Finally, the structural features uncovered in this work have direct implications for material properties and applications. The heterogeneous internal organization observed in the spherical aramid particles is consistent with their enhanced thermal stability and chemical resistance, as evidenced by their robustness against concentrated sulfuric acid and high-temperature degradation. This suggests that internal organization and mesoscale structure, rather than bulk packing alone, may influence functional performance. More broadly, the ability to tune morphology, packing density, and internal organization through diffusion--reaction competition opens pathways to hierarchical polymer architectures with tailored mechanical, thermal, and transport properties, providing a basis for the rational design of hierarchical polymer architectures under non-equilibrium conditions.[13]

Methods

Materials and polymerization

Aromatic polyamide and related polymer particles were synthesized via phase-transition polymerization using C_3-symmetric monomers with different reactive functional groups. In this method, polymerization proceeds through a phase transition of the growing polymer, which governs structural evolution under diffusion–reaction competition.

The total amount of monomers was fixed at 2 g, and the monomers were introduced at equimolar ratios to give a concentration of 10 wt% in the reaction mixture.

Representative systems include reactions based on benzene-1,3,5-tricarboxylic acid and 1,3,5-benzene triacetamide, yielding TPA–DBT and TPA–IL structures using dibenzyltoluene (DBT) and the ionic liquid 1-butyl-3-methylimidazolium hexafluorophosphate (BMIM–PF_6) as solvents, respectively. Another system involves the reaction between 1,3,5-tris(4-carboxyphenyl)benzene and 1,3,5-tris(4-aminophenyl)benzene, forming TTPA–IL structures. The other system involves the reaction between 1,3,5-tris(4-carboxyphenyl)benzene and 1,3,5-tris(4-hydroxyphenyl)benzene, forming TTPE–IL structures via ester linkage formation. As lower-reactivity control systems, reactions based on benzene-1,3,5-tricarboxylic acid with melamine and with phloroglucinol were performed in BMIM–PF_6, yielding TPMA and TPE, respectively.

In a typical procedure, the monomer-containing phases were combined under vigorous

stirring (300 rpm) in a 100 mL flask, enabling phase-transition polymerization under diffusion–reaction-controlled conditions.

The reaction was carried out at 200 °C for 24 h in the ionic liquid system at a concentration of 10 wt%, and at 340 °C for 8 h in dibenzyltoluene (DBT) at 1 wt%, leading to the formation of polymer particles at the interface. The difference in reaction temperature reflects differences in solvent stability and reaction environments between the ionic liquid and DBT systems.

The resulting products were collected by filtration, thoroughly washed with methanol for the ionic liquid system and with acetone for the DBT system to remove residual monomers, and dried under vacuum prior to characterization.

Control experiments were conducted using lower-reactivity monomers such as melamine and phloroglucinol under identical conditions.

Density Measurement

True density was measured using a helium pycnometer after drying the samples under vacuum. Multiple measurements (n>5) were performed to ensure reproducibility.

Morphological characterization

Scanning electron microscopy (SEM) was performed to examine particle morphology using a JEOL JSM-6701F instrument and an acceleration voltage of 5 kV. Dry powder samples were placed on carbon-coated Cu TEM grids (ELS-C10, Okenshoji Co., Ltd.) and lightly tapped to remove loose particles prior to observation.

Scanning transmission electron microscopy (STEM–SEM) imaging was conducted to evaluate internal structure via contrast differences between the particle shell and interior. Dry powder samples were prepared in the same way as the SEM samples before observation by STEM (Quattro S, Thermo Fisher Scientific) at an acceleration voltage of 30 kV.

Focused ion beam–scanning electron microscopy (FIB–SEM) was used to obtain cross-sectional images of individual particles, enabling direct observation of multilayered internal architectures. Cross-sectional samples were prepared using a focused ion beam and imaged in a Carl Zeiss Gemini 560 microscope at an accelerating voltage of 1 kV.

Structural characterization

Powder X-ray diffraction (XRD) measurements were carried out at room temperature using a Rigaku RINT-TTR3 diffractometer with Cu Kα radiation ($\lambda = 1.5418$ Å), operated at 40 kV – 300 mA to evaluate molecular packing and lamellar spacing.

Polarized optical microscopy (POM) was carried out using a Nikon Eclipse LV100POL microscope to examine birefringence and morphological features during and after particle formation.

Small-angle X-ray scattering (SAXS) and wide-angle X-ray scattering (WAXS) measurements were performed at the BL38B1 beamline in SPring-8 to investigate mesoscale structural organization in TTPA–IL. Samples were loaded into 1.5 mm borosilicate glass capillaries and measured using an incident X-ray energy of 12.4 keV (λ = 1.0 Å). The sample-to-detector distance was 2.6 m for SAXS measurements and 0.2 m for WAXS measurements. Data were collected at ten different points with 5 s exposure each with a DECTRIS PILATUS3X 2M detector. The acquired data were averaged and subsequently corrected by subtracting dark-current and background using the XSACT software [17]. Correlation-function analysis was performed to estimate characteristic mesoscale structural dimensions, including hard-domain size and long-period correlation lengths. Correlation-function analysis was performed using SASView software to estimate characteristic hard-domain sizes and long-period correlations from the SAXS profiles.[18]

Chemical and thermal stability

The chemical stability of the particles was evaluated by dispersing samples in concentrated sulfuric acid and observing structural changes using polarized optical microscopy under crossed-Nicol conditions.

Thermogravimetric analysis (TGA) was performed under both inert (100% Ar) and oxidative (80% Ar: 20% O_2) atmospheres at a heating rate of 10 °C/min to evaluate thermal stability of the polymers.

Reproducibility

All measurements were performed on independently prepared samples, and key experiments were repeated to confirm reproducibility.

Funding

This work was supported by the RIKEN–Sumitomo Chemical collaborative research program.

Acknowledgements

We gratefully acknowledge Professor Junji Watanabe for his insightful advice encouraging us to explore polymers, which significantly influenced the direction of this

study. We also thank Gurvan Bosser and Dr. Daishi Inoue for their valuable assistance with powder X-ray diffraction (pXRD) and STEM-SEM measurements, respectively. We further thank Dr. Priyanka Sharma for valuable discussions and assistance with SAXS measurements and data analysis. The authors thank TRIP-Polymer Science Use Case for SAXS measurements at SPring-8 under the project No. 20260064, and R-COMS_CEMS for pXRD and STEM-SEM.

Author Contributions

S.O. conceived and supervised the project. S.O. and J.L. designed the experiments and analyzed the data. S.O. performed the synthesis and J.L. performed structural characterization. S.O. wrote the manuscript with input from all authors. All authors discussed the results and contributed to the final version of the manuscript.

Competing Interests

S.O. is an inventor on a patent application related to the materials described in this work. All other authors declare no competing interests.

Data reproducibility

All measurements were performed using independently prepared samples, and representative data are shown unless otherwise stated.

References

1. Ugarte, D. Curling and closure of graphitic networks under electron-beam irradiation. Nature 359, 707–709 (1992).

2. McDonough, J. K. & Gogotsi, Y. Carbon onions: synthesis and electrochemical applications. Electrochem. Soc. Interface 22, 61–66 (2013).

3. Boulanger, L., Andriot, B., Cauchetier, M. & Willaime, F. Concentric shelled and plate-like graphitic boron nitride nanoparticles produced by CO_2 laser pyrolysis. Chem. Phys. Lett. 234, 227–232 (1995).

4. Tenne, R., Margulis, L., Genut, M. & Hodes, G. Polyhedral and cylindrical structures of tungsten disulfide. Nature 360, 444–446 (1992).

5. Zink, N., Therese, H.A., Pansiot, J., Yella, A., Banhart, F. & Tremel, W., In Situ Heating TEM Study of Onion-like WS2 and MoS2 Nanostructures Obtained via MOCVD. Chem. Mater. 20, 65-71 (2008).

6. Ensafi, A. A., Moosavifard, S. E., Rezaei, B. & Kamari Kaverlavani, S. Engineering onion-like nanoporous $CuCo_2O_4$ hollow spheres derived from bimetal–organic

frameworks for high-performance asymmetric supercapacitors. J. Mater. Chem. A 6, 10497-10506 (2018).

7. Okamoto, S., Llandro, J., Gibbons, A., Arfaoui, M., Hashizume, D. & Watanabe, J. Orthogonal staggered alignment of molecular chains in aramid whiskers: a game-changer for sustainable, high-performance composites. Macromol. Rapid Commun. 47, e00919 (2026).

8. Okamoto, S., Llandro, J., Ikeda, J. & Watanabe, J. Perpendicular chain orientation in poly(para-benzamide) single-crystal nanowhiskers for enhanced dispersibility. ACS Appl. Nano Mater. 9, 7330–7338 (2026).

9. Okamoto, S., Llandro, J., Teng, K.-F., Chang, P., Liang, K., Arfaoui, M., Hashizume, D. & Watanabe, J. Microbially derived p-aminobenzoic acid for poly(p-benzamide) whiskers: the influence of monomer synthetic routes on crystallization and thermal behavior. *React. Funct. Polym.* **227**, 106868 (2026).

10. Zarket, B. C. & Raghavan, S. R. Onion-like multilayered polymer capsules synthesized by a bioinspired inside–out technique. Nat. Commun. 8, 193 (2017).

11. Ramli, R. A. Hollow polymer particles: a review. RSC Adv. 7, 52632–52650 (2017).

12. Okubo, M., Minami, H., Morikawa, Y. & Saito, K. Polymer hollow particles with controllable holes in their surfaces. Nat. Mater. 4, 811–815 (2005).

13. Fogler, H. S. Elements of Chemical Reaction Engineering, 6th ed. (Pearson, 2020).

14. Bañuelos, J. L., Elizalde-Solis, O., Cazares-Marinero, J. J., Cortés-Arriagada, D., Ifuku, S., Román-Velázquez, C. E. & Martínez-Magadán, J. M. Densification of ionic liquid molecules within a hierarchical nanoporous carbon structure revealed by small-angle scattering and molecular dynamics simulation. Chem. Mater. 26, 1144–1153 (2014).

15. Bale, Harold D., and Paul W. Schmidt. "Small-angle X-ray-scattering investigation of submicroscopic porosity with fractal properties." *Physical Review Letters* 53, no. 6 (1984): 596.

16. Du, Ai, Yuhan Xie, Yan Li, Yongdong Pan, Guangming Wu, and Bin Zhou. "Ultra-slow sound in non-resonant meta-aerogel." *arXiv preprint arXiv:2003.09059* (2020).

17. XSACT: X-ray Scattering Analysis and Calculation Tool." SAXS & WAXS data analysis software — Version 3.1., Xenocs, 2025.

18. J. Krzywon et al. SasView Version 6.1.2, 10.5281/zenodo.17795298

Supplementary Files

This is a list of supplementary files associated with this preprint. Click to download.

- SupportingInformation.docx